Unusual modes and photonic gaps in a Vicsek waveguide network

Sheelan Sengupta and Arunava Chakrabarti
Department of Physics, University of Kalyani, West Bengal 741 235, India.

Abstract

We propose a simple model of a waveguide network designed following the growth rule of a Vicsek fractal. We show, within the framework of real space renormalization group (RSRG) method, that such a design may lead to the appearance of unusual electromagnetic modes. Such modes exhibit an extended character in RSRG sense. However, they lead to a power law decay in the end-to-end transmission of light across such a network model as the size of the network increases. This, to our mind, may lead to an observation of power law localization of light in a fractal waveguide network. The general occurence of photonic band gaps and their change as a function of the parameters of the system are also discussed.

PACS: 42.25.Bs, 42.82.Et, 61.44.Br, 72.15.Rn

1 Introduction

Propagation of electro-magnetic waves in dielectric materials has received extensive attention in recent years [1]-[7]. The existence of photonic band gaps (PBG) in the transmission spectra of such materials is of particular interest and is of importance in both fundamental science and technological applications. These studies constitute principal part of mesoscopic physics, a major focus being the possibility of localization of light [5, 6], a direct evidence of which has already been reported for a strongly scattering media of semiconductor powders [7]. The localization of classical waves is purely a result of multiple scattering in a random environment and free from the complications arising from interaction effects. Though, due to Rayleigh scattering, it is more difficult to localize classical waves compared to electrons.

An alternative to the usual PBG systems may be obtained by forming network with slender waveguide tubes. This geometry does not need materials with high dielectric constants and yet, is capable of demonstrating Anderson localization of light. Zhang et al [8] have experimentally observed Anderson localization of light in a three dimensional network consisting of nearly one dimensional segments of waveguide. Vesseur et al [9] have examined the photonic band structure of a comb-like waveguide geometry. This work provides an example of a one dimensional photonic crystal enabling one to investigate the occurrence of localized states in such systems. The network system can produce large gaps even in one dimension, though it may

be sensitive to the structure of the unit cell. Recently, network models using serial loop structure have been studied in the context of propagation of electro-magnetic and acoustic waves [10, 11]. Such theoretical investigations are additional justified as the present day nano-technology produce tailor-made waveguide networks with different geometries.

Photonic band gaps also exist in the network systems without periodicity, such as fractal networks [12]. Due to their self-similar structures and the absence of translational invariance within the structures, fractals [13, 14] are much more complicated to study compared to the periodic systems. Investigation of the propagation of classical waves in a network model designed following a fractal geometry offers an interesting opportunity to observe the interplay of deterministic but non-translational order and interference effects. Unfortunately, this aspect has been grossly overlooked in the literature except for the recent work done by Li et al [12], on a Sierpinski gasket network.

In the present work, we propose a model waveguide network based on the geometry of a Vicsek fractal [15]-[17]. We study the transmission of electromagnetic waves through finite sized Vicsek Waveguide Network (VWN) using real space renormalization group (RSRG) and transfer matrix (TM) methods. A regular Vicsek fractal is already known to possess exotic spectral properties [15]-[17]. In addition to this, it has also been seen shown that an infinite Vicsek fractal can support a countable infinity of extended wavefunction in the context of electronic transport [18, 19]. Some of these states are 'anomalous' in the sense that the behaviour of the RSRG flow of the parameters of the system and the electronic transport are incompatible to each other [19]. This acts as an additional motivation for our work. We wish to examine the appearence of photonic gaps in such a network system, the dependence of the gaps on the system size and the possible occurence of extended electromagnetic modes in such a deterministic fractal network.

We find interesting spectal behaviour and formation of photonic gaps in a VWN. Additionally, we have been able to discern a number of eigenmodes in a VWN, some of which display a completely extended nature. For this latter set of states, the RSRG flow of the parameters gives a signature of extendedness, while the end-to-end light transmission decays following a power law as a function of the size of the network. This, to our mind, may lead to a possible power law trapping of light from an experimental point of view. We present out results below.

2   The model and the method

A 'unit cell' of a simple Vicsek geometry is obtained by considering a 'cross' with four dangling ends [17] joined at a node, as a building unit. The next generation
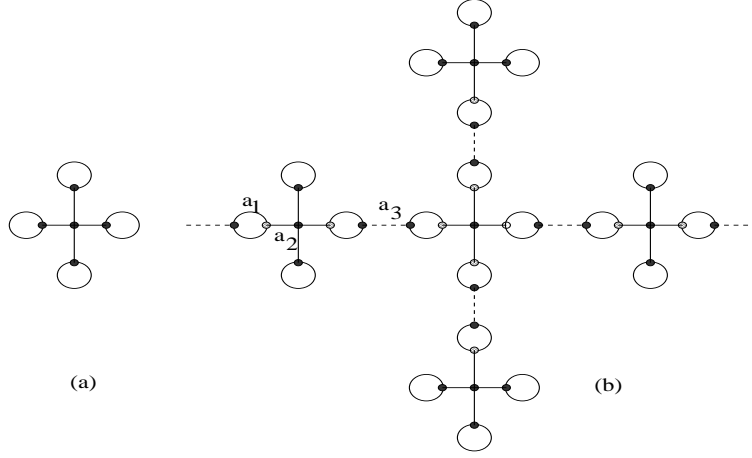
Figure 1: Vicsek waveguide network in the (a) first and (b) second generation. The loops are attached to the open ends of a unit 'cross' as shown in (a). The patterned circles represent the nodes which are 'decimated' to obtain a Vicsek lattice of points.

fractal is obtained by placing four such 'crosses' around a central cross and so on [17]. A VWN may be constructed by considering each arm of a 'unit' cross to be consisting of a one dimensional waveguide segment. The dangling edges cause problems in realizing the boundary conditions from the standpoint of experiments. So, we attach loops of the same waveguide material at each end of a dangling arm. The first and the second generation VWN thus resemble what have been illustrated in Fig. 1. Each arm of a loop is of length a_1. The other segments are of lengths a_2 and a_3 as shown in Fig. 1.

Following Zhang and Sheng [20] the 'wave-function' $\psi_{i,i+1}$ within any segment of length $l_{i,i+1}$ between the nodes i and $i+1$ is given by,

$$\psi_{i,i+1}(x) = \psi_i \frac{\sin[k(l_{i,i+1} - x)]}{\sin k l_{i,i+1}} + \psi_{i+1} \frac{\sin kx}{\sin k l_{i,i+1}} \tag{1}$$

where, ψ_i is the amplitude at the ith node, and k is the absolute value of the wave vector in the loop. For an electromagnetic wave, $k = \frac{i\omega\sqrt{\epsilon}}{c_0}$ where ω and c_0 are the frequency and the speed (in vacuum) of the electromagnetic wave respectively. ϵ is the relative permittivity of the dielectric medium, which we may assume to be real. A complex dielectric constant can easily be dealt with. The continuity of the wave function at the nodes and the flux conservation criterion are used to map the problem of wave propagation in such loops into an equivalent tight binding problem of electron propagation on a one dimension lattice [20].The resulting difference equation is,

$$(E - \epsilon_i)\psi_i = t_{i,i+1}\psi_{i+1} + t_{i-1,i}\psi_{i-1} \tag{2}$$

3

Here, we parametrize $E = 2 \cos k l_{i,i+1}$ and, define an effective on-site potential

$$\epsilon_i \;=\; 2 \cos k l_{i,i+1} + \sum_{m=1}^{N_{i,i-1}} \cot \theta_{i-1,i}^{(m)} + \sum_{m=1}^{N_{i,i+1}} \cot \theta_{i,i+1}^{(m)} \tag{3}$$

and the effective nearest neighbour 'hopping integral' is given by,

$$t_{i,i+1} = \sum_{m=1}^{N_{i,i+1}} \frac{1}{\sin \theta_{i,i+1}^{(m)}} \tag{4}$$

where, $N_{i,i\pm1}$ is the number of segments between the nodes i and $i\pm1$. $\theta_{i,i+1}^{(m)} = k l_{i,i+1}^{(m)}$ is the corresponding phase acquired in the mth segment. The problem of wave propagation now becomes mathematically equivalent to the problem of transmission of an electron with energy E through the mapped lattice, where, $-2 \leq E \leq 2$.

It is now simple to eliminate the amplitudes ψ_i corresponding to the nodes denoted by the patterned circle in [Fig. 1(b)] in terms of the amplitudes at the remaining sites. The result is a Vicsek lattice of points [Fig. 2(a)]. In the equivalent language of the electronic problem, we now have three distinct values for the on-site potentials, given by,

$$
\begin{aligned}
\epsilon_A &= 2 \cos \theta_3 + 2 \cot \theta_1 + \cot \theta_2 + \frac{4}{\sin^2 \theta_1} \left(\frac{1}{E - 2 \cos \theta_3 - 2 \cot \theta_1 - \cot \theta_2} \right) \\
\epsilon_B &= 2 \cos \theta_3 + \cot 2\theta_1 + \cot \theta_2 \\
\epsilon_C &= 2 \cos \theta_3 + 4 \cot \theta_1 + \frac{2}{\sin^2 \theta_2} \left(\frac{1}{E - 2 \cos \theta_3 - 2 \cot \theta_1 - \cot \theta_2} \right)
\end{aligned}
\tag{5}
$$

and, the three nearest neighbour 'hopping integrals' are given by:

$$
\begin{aligned}
t_1 &= \frac{2}{\sin \theta_1 \sin \theta_2} \left(\frac{1}{E - 2 \cos \theta_3 - 2 \cot \theta_1 - \cot \theta_2} \right) \\
t_2 &= \frac{1}{\sin \theta_2} \\
T &= \frac{1}{\sin \theta_3}
\end{aligned}
\tag{6}
$$

where, T is the n.n. hopping integral between two neighbouring clusters. Here, $2a_1$, a_2, a_3 are the lengths of the loop, the wire and the connector connecting the two neighbouring clusters respectively. Therefore, $\theta_j = k a_j$ with $a_j = a_1, a_2, a_3$. This reconstruction facilates the use of RSRG to discern the extended and other modes of the lattice as well as to compute the transmittivity. The results are now discussed.

3   Unusual eigenmodes of a VWN

Let us consider a VWN at any arbitrary generation (converted into a Vicsek lattice, of points) clamped between two semi-infinite waveguide leads. Such a construction
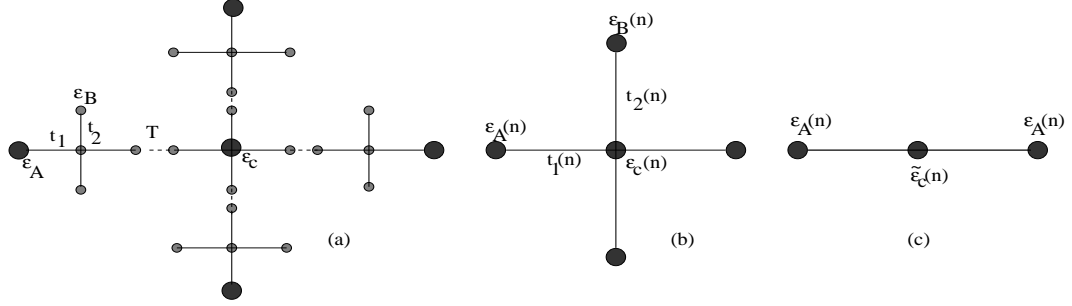
Figure 2: (a) A second generation VWN transformed into a Vicsek lattice of points on elimination of the patterned circles in Fig 1. The effective (renormalized) on-site potentials and hopping integrals are shown. (b) The one-step renormalized lattice obtained from (a). (c) The final triatomic molecule to be placed between the leads.

in its second generation is shown in Fig 3. Now, a VWN at any generation $n + 2$ can be renormalized n times to obtain a second generation structure by decimating the appropriate vertices [19]. The RSRG recursion relations for the on-site terms and the hopping integrals are given by,

$$
\begin{aligned}
\epsilon_A(n+1) &= \epsilon_A(n) + \frac{t_1^2(n)}{E - F_2(n)} \\
\epsilon_B(n+1) &= \epsilon_B(n) + \frac{t_2^2(n)}{E - F_2(n)} \\
\epsilon_C(n+1) &= \epsilon_C(n) + 4t_1^2(n)F_4(n) \\
t_1(n+1) &= \frac{t_1^3(n)T(n)F_1(n)}{[E - \epsilon_A(n)][E - F_2(n)]} \\
t_2(n+1) &= \frac{t_2(n)t_1^2(n)T(n)F_1(n)}{[E - \epsilon_A(n)][E - F_2(n)]} \\
T(n+1) &= T(n)
\end{aligned}
\tag{7}
$$

where, n denotes the stage of renormalization and

$$
\begin{aligned}
F_1(n) &= \frac{E - \epsilon_A(n)}{[E - \epsilon_A(n)]^2 - T^2(n)} \\
F_2(n) &= \epsilon_C(n) + \frac{2t_2^2(n)}{E - \epsilon_B(n)} + t_1^2(n)F_1(n) \\
F_3(n) &= \frac{E - \epsilon_B(n)}{[E - \epsilon_B(n)][E - \epsilon_C(n)] - 2t_2^2(n)} \\
F_4(n) &= \frac{E - \epsilon_A(n) - t_1^2(n)F_3(n)}{[E - \epsilon_A(n)][E - \epsilon_A(n) - t_1^2(n)F_3(n)] - T^2(n)}
\end{aligned}
$$
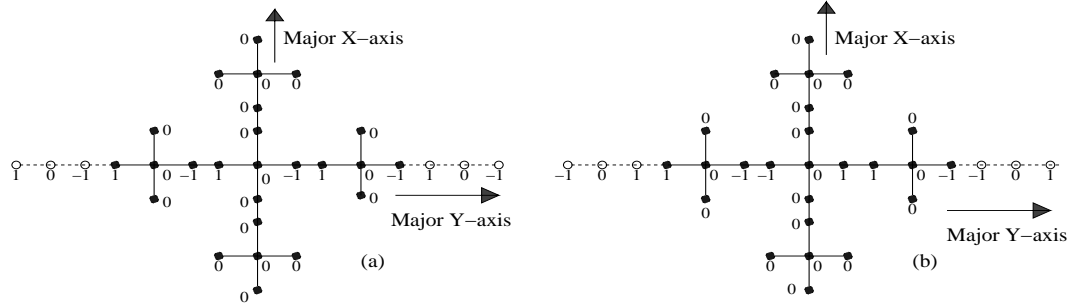
It is seen that T remains fixed under RSRG iterations.

Figure 3: Distribution of amplitudes of the 'extended' wavefunction for the lead (dashed lines)-sample-lead systems corresponding to (a)$E = \epsilon_A - T$ and (b) $E = \epsilon_A + T$. The transmission corresponding to these states across the sample decays with increasing system size as explained in the text.

It is not difficult now to construct, by inspection, extended wave functions which have non trivial distribution of amplitudes along the X-axis. The wave vectors for these wavefunctions are obtained by setting

$$E = \epsilon_A(n) \pm T \tag{8}$$

As the RSRG process can proceed, in principle indefinitely, one can extract an infinity of different k-values by solving the equation (8). A couple of such states are illustrated in Fig. 3 on a second stage fractal for $E = \epsilon(n) \pm T$. It should be noted that ϵ_C in general flows to infinity with the progress of re-normalization. Therefore, it is necessary to choose the amplitudes at the central site of all the basic five-site cells to be zero in order to avoid the divergence of amplitudes at any arbitrary site. The 'extended' character of these eigenmodes are usually tested from a study of the flow of the 'hopping integrals' under successive RSRG steps.

The recursion relations (7) reveal that if, $E = \epsilon_A(n) - T$ at any nth stage of re-normalization, then ϵ_A, ϵ_B, t_1 and t_2 immediately reach their fixed points i.e. $\epsilon_A(n+1) = \epsilon_A(n)$, $\epsilon_B(n+1) = \epsilon_B(n)$, $t_1(n+1) = t_1(n)$ and $t_2(n+1) = t_2(n)$ for all subsequent stages of renormalization. This implies that at any scale of length there is a nonzero overlap between the wave-functions at the nearest neighbour sites (at that scale), and that the amplitudes remain finite everywhere in even an infinite lattice. For example, solving $E = \epsilon_A - T$ we get $ka = 0.547457038567240$ and 2.118253365362137 with $a_1 = a_2 = a_3 = a = 1$. The hopping integrals t_1 and t_2 remain fixed at nonzero values (corresponding to their fixed points) in these two cases. Thus, from an RSRG point of view we expect an extended character of such states. To see whether such states are 'transparent' in regard of the incoming wave, we have to compute the transmission of an electromagnetic wave incident on a finite VFN through leads connected to the two-ends of the fractal lattice.

6

4   Transmission coefficient

4.1   Formulation

To calculate the transmission coefficient we first renormalize the Vicsek lattice n-times using the RSRG decimation method. The result is a Vicsek lattice consisting of five vertices and characterized by the n-times renormalized values of the 'on-site' potentials and the 'hopping integrals'. The recursion relations are given by Eq. (7). This renormalized version [Fig. 2(b)] is now reduced to a 3-site cluster [Fig. 2(c)] and the effective on-site potential of the central site becomes

$$\tilde{\epsilon}_C(n) \;=\; \epsilon_C(n) + \frac{2t_2^2(n)}{E - \epsilon_B(n)} \tag{9}$$

This triatomic 'molecule' is now clamped between two semi-infinite perfect waveguides, which are represented, following the discretization process outlined in Ref [20], by a sequence of identical site potentials

$$\epsilon_0 = 2\cos\theta_3 + 2\cot\theta_3 \tag{10}$$

and nearest neighbour hopping integral

$$t_0 = \frac{1}{\sin\theta_3} \tag{11}$$

The decimation procedure is illustrated in Fig. 2 for a second generation fractal. The equations are easily obtained by artificially considering the lead to be consisting of identical materials of length a_3 joined end-to-end. The transmission coefficient τ is now given by [21],

$$\tau = \frac{4\sin^2\theta_3}{[P_{12} - P_{21} + (P_{11} - P_{22})\cos\theta_3]^2 + (P_{11} + P_{22})^2\sin^2\theta_3} \tag{12}$$

where,

$$P_{11} \;=\; \frac{[E - \epsilon_A(n)]^2[E - \tilde{\epsilon}_C(n)]}{t_1^2(n)t_0} - \frac{2[E - \epsilon_A(n)]}{t_0}$$

$$P_{12} \;=\; 1 - \frac{[E - \epsilon_A(n)][E - \tilde{\epsilon}_C(n)]}{t_1^2(n)}$$

$$P_{21} \;=\; -P_{12}$$

$$P_{22} \;=\; -\frac{t_0[E - \tilde{\epsilon}_C(n)]}{t_1^2(n)}$$

4.2   Results

(a) Let us analyze the wavefunction which corresponds to an extendedd state of the lead-VWN-lead system. For the values of wave vector correspond to the energy
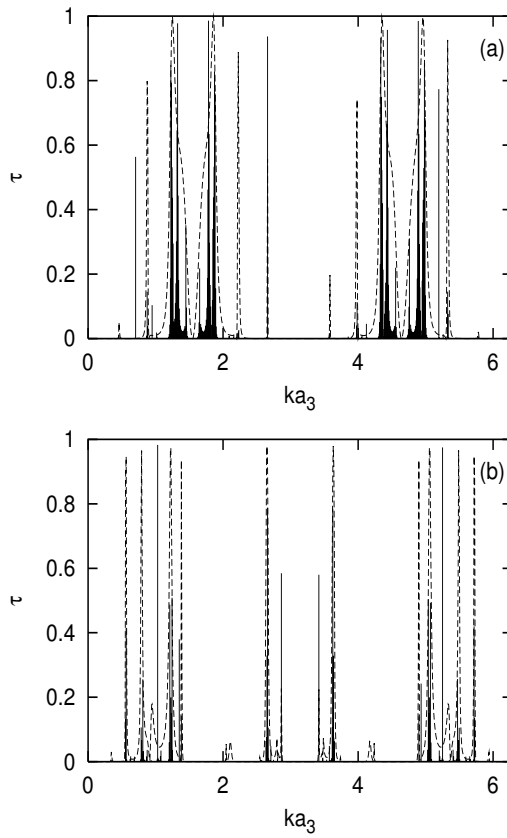
Figure 4: (a) τ vs ka_3 with $a_1 = 0.01$, $a_2 = a_3 = 1$. (b) $a_1 = 0.05$, $a_2 = a_3 = 1$. The solid and the dashed lines in each figure indicate results for the second and the first generation VWN respectively.

$E = \epsilon_A - T$, for example, we can use the recursion relations (7) to write explicitly the renormalized values of ϵ_C in the successive generations as,

$$\epsilon_c(1) = 5\epsilon_c - \sigma$$

$$\epsilon_c(2) = 5^2\epsilon_c - 5\sigma - \sigma$$

and so on. Here

$$\sigma = 4(\epsilon_A - T) - \frac{8t_2^2}{\epsilon_A - \epsilon_B - T} + \frac{4t_1^2}{T}$$

is constant because ϵ_A, ϵ_B, t_1, t_2 and T attain their fixed point values for $n \geq 1$. Continuing in this way we get, after n steps of renormalization,

$$\epsilon_c(n) = 5^n\epsilon_c - P_{n-1}(\sigma)$$

where,

$$P_{n-1}(\sigma) = 5^{n-1}\sigma + 5^{n-2}\sigma + \text{...........} + \sigma$$

and $5^n = N$, the system size of the lattice at its nth generation. Therefore, we see that for large values of n, i.e., for large size of the original lattice $\epsilon_C(n) \sim N$ as ϵ_A, ϵ_B, t_1 and t_2 are invariant at each step of renormalization. So for large n, its simple to work out from Eq. (8) that $\tau \sim \frac{1}{N^2}$ indicating power law decay as a function of the total number of matrices. This is incompatible with the invariance of the hopping integrals under RSRG. The growth of $\epsilon_C(n)$ under RSRG implies that an electromagnetic wave travelling through the perfect waveguide leads and entering the fractal structure will experience larger and larger effective 'potentials' at the centres of the five site clusters. For large enough VWN systems we thus have the possibility of a power law localization of light.

The existence of the dangling side units consisting of a wire and a loop which themselves form a fractal geometry, causes destructive interference between the waves propagating and reflecting back and forth along these side units. As for all these wave vectors the amplitude of the wave function is pinned at the value zero at the centerers of five site clusters at different length scale, standing waves are formed along the branches with nodes at the centers of one or the other five site cluster, which should localize the light wave and reduce the transmission. We call such modes 'unusual', and emphasize that these are eigenmodes not for a finite cluster, but for the *lead-VWN-lead system*, irrespective of its size.

(b) We have also examined the features of the transmission spectrum of finite VWN's of arbitrary size. The appearance of transmission maxima separated by photonic gaps is a general phenomenon. The fragmentation in the spectrum increasing with increasing size of the system. Figures (4) and (5) exhibit the main characteristics where, in addition to the variation of τ against the wave vector, we study the effect of the change of the size of the loops (a_1). Three cases have been explicitly
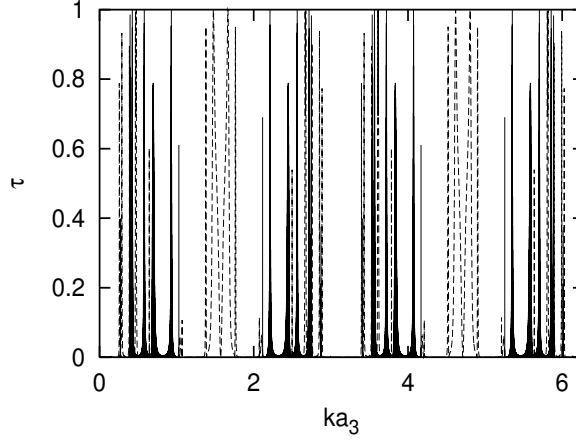
Figure 5: τ vs ka_3 with $a_1 = 2$, $a_2 = a_3 = 1$. The solid and the dashed lines now represent the results for the first and the second generation VWN respectively. The appearance of new transmission zones is clearly seen between $ka_3 = 0$ and 2, 4 and 6.

shown with the size of the loop (a_1) increasing from a very small value to a value comparable to the lengths of the other waveguide segments (a_2 and a_3).

Though in every case, the exact distribution of values of the *tau* is sensitive to the individual values of the parameters, still some interesting behaviour is observed in certain cases. For example, setting $a_2 = a_3 = 1$ and $a_1 = 0.01$ in arbitrary units, the transmission spectrum shows the presence of clusters of high transmittivity flanked by sharp delta-like peaks, even for a first generation VWN [dashed line in Fig. 4(a)]. The same set of parameters leads to a fragmented band structure as we move over to the second generation [vertical line in Fig. 4(b)]. The spectrum reveals almost similar features as a_1 is gradually increased from 0.01 to higher values. For $a_1 = 0.5$, we get a clear signature of wider photonic gaps separating four clusters of high transmittivity. This is seen in Fig. 4(b), where the dashed and the solid lines again correspond to the first and second stage VWN.

When the dimension of the loop starts getting larger than the connecting waveguide segments, we find that new clusters of transmission maxima start appearing in the major photonic gaps of the earlier generation [Fig. 5]. The three major photonic gaps corresponding to the first generation fractal get populated by two major photonic bands (dashed line in Fig. 5) when the length of the loop exceeds the other two segments a_2 and a_3.

To make the appearance of the photonic gaps more pronounced, in Fig. 6 we show the variation of transmission coefficient τ of a VWN in the first (dashed curve) and the second (solid vertical lines) respectively. The more or less fixed zones of
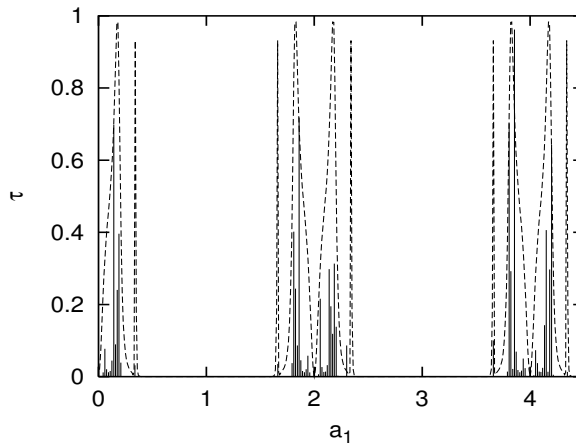
10

Figure 6: τ vs a_1 with $a_2 = a_3 = 1$ and $k = \pi/2$.

zero transmission around $a_1 = 1$ and $a_1 = 3$ mark the broad photonic band gaps in a VWN.

5 Conclusion

We have shown that light transmission in a Vicsek fractal geometry is marked by the appearance of unusual extended-like eigenmodes for which a non-trivial distribution of finite amplitudes can be obtained in a Vicsek waveguide network clamped between semi-infinite leads. The transmittivity of such a lead-network -lead system shows a power law decay as the network grows bigger. Broad photonic gaps are obtained by appropriately choosing the network parameters.

References

[1] *Photonic band gap materials*, edited by C. M. Soukoulis (Kluwer, Dordrecht, 1995).

[2] S. John, Phys. Rev. Lett. 58 (1987) 2486.

[3] E. Yablonoviteh, Phys. Rev. Lett. 58 (1987) 2059.

[4] M. S. Schwa, Int. J. Mod. Phys. B 10 (1996) 977.

[5] D. Z. Zhang, W. Wu, Y. L. Zhang, L. Li, B. Y. Cheng, G. Z. Yang, Phys. Rev. B 50 (1994) 9810.

[6] S. L. Macall, P. M. Platzman, R. Dalichaouch, D. Smith, S. Schultz, Phys. Rev. Lett. 67 (1991) 2017; Nature (London) 354 (1991) 53.

[7] D. S. Wiersma, P. B. artolini, Ad. Lagendijk, R. Righini, Nature (London) 390 (1997) 671.

[8] Z. Q. Zhang, C. C. Wong, K. K. Fung, Y. L. Ho, W. L. Chan, S. C. Kar, T. L. Chan, N. Cheung, Phys. Rev. Lett. 81 (1998) 5540.

[9] J. O. Vesseur, B. Djafari-Rouhani, L. Dobrzynski, A. Akjouj, J. Zemmouri, Phys. Rev. B 59 (1999) 13446.

[10] A. Mir, A. Akjouj, J. O. Vesseur, B. Djafari-Rouhani, N. Fethouhi, E. H. El Boudouti, L. Dobrzynski, J. Zemmouri, J. Phys.: Condens. Matt. 15 (2003) 1593.

[11] A. Akjouj, H. Al-Wahsh, B. Sylla, B. Djafari-Rouhani, J. Phys.:Condens. Matt. 16 (2004) 37.

[12] M. Li, Y. Liu, Z-Qing Zhang, Phys. Rev. B 61 (2000) 16193.

[13] E. Domany, S. Alexznder, D. Bensimon, L. P. Kadanoff, Phys. Rev. B 28 (1983) 3110.

[14] R. Rammal, G. Thoulous, Phys. Rev. Lett. 49 (1982) 1194.

[15] C. S. Jayanthi, S. Y. Wu, Phys. Rev. B 48 (1993) 10188.

[16] C. S. Jayanthi, S. Y. Wu, Phys. Rev. B 48 (1993) 16193.

[17] J. Q. You, C. Lam, F. Nori, L. M. Sander, Phys. Rev. E 48 (1993) R4183.

[18] A. Chakrabarti, Jour. Phys.: Condens. Matt. 8 (1996) L99.

[19] A. Chakrabarti, B. Bhattacharyya, Phys. Rev. B 54 (1996) R12625.

[20] Z. Q. Zhang, P. Sheng, Phys. Rev. B 49 (1994) 83.

[21] A. Douglas Stone, J. D. Joannopoulos, D. J. Chadi, Phys. Rev. B 24 (1981) 5583.